Proceedings of the 23rd International Congress on Applications of Lasers and Electro-Optics 2004

USE OF DIC IMAGING IN EXAMINING PHASE TRANSFORMATIONS IN DIODE LASER SURFACE HARDENING

Henrikki Pantsar

Laser Processing Laboratory, Lappeenranta University of Technology
Lappeenranta, Finland

Abstract

Processing parameters in Laser Transformation Hardening have a great effect on microstructures produced via phase transformations. In order to establish the effects for a wide range of processing parameters a large amount of specimens has to be processed and examined by microstructural analysis from polished and etched samples. The process is time consuming and therefore the number of processed samples is often minimized. In the presented study polished surfaces of low alloy steel and plain carbon steel samples have been hardened in an inert gas atmosphere using a HPDL (High Power Diode Laser) beam. Surface relief formed during phase transformations has been photographed using DIC (Differential Interference Contrast) imaging. The effect of processing parameters on austenitization, microstructure and extent of martensitic transformation has been investigated. The hardness of each sample is measured. Experiments show that DIC imaging is a rapid and illustrative tool for microstructural analysis of iron-based material processing.

Introduction

Laser transformation hardening (LTH) is a process in which phase transformations in steels are induced by irradiating the surface with a laser beam. Surface regions are heated to temperatures above the A_{c1} transformation temperature, resulting in austenitization. A schematic sketch of the transformation hardening process of hypo-eutectoid steel with laser irradiation is presented in Figure 1. The surrounding material acts as an efficient heat sink. Heat is transported away from the surface by thermal conduction, inducing rapid cooling. Austenitized material, provided with sufficient quantities of carbon, forms martensite on quenching, producing a hard and wear resistant surface. The properties of the hardened layer are controlled by the energy input, which depends on the beam power density and interaction time. Long interaction times enable more heat to be conducted into the material before the melting temperature is attained at the surface, thus producing a deeper hardened layer. A higher traverse rate and higher power density results in higher cooling rate, at the expense of the depth of the hardened layer.

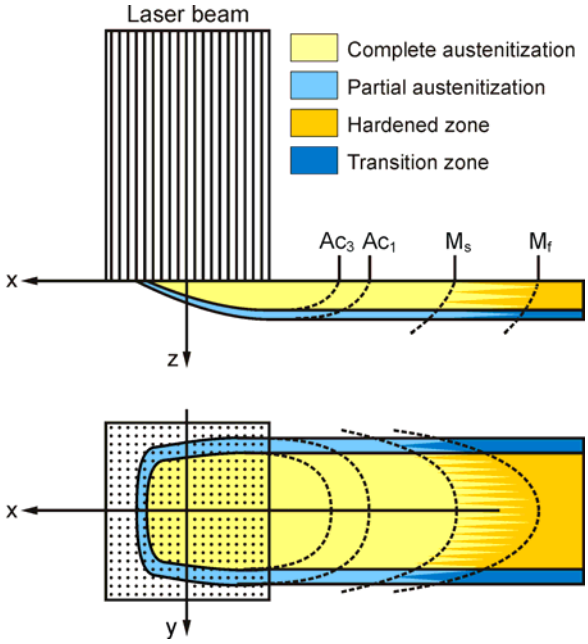

Figure 1. A schematic sketch of the transformation hardening process with laser irradiation.

The geometry of the hardened layer depends on the processing parameters and beam-matter interaction, and their effect on the thermal cycle induced by laser radiation. Consequent phase transformations, which determine the hardness of the resulting microstructure, are affected by the material composition, initial microstructure and processing parameters. Since the combined effect of these factors is demanding to estimate, a break down analysis is presented in the following chapters in order to indicate the influence of these constituents separately.

Phase Transformations During Laser Transformation Hardening

The aim of laser transformation hardening is to produce a hard, wear resistant surface in discrete areas of a component. In this aspect martensite *α'* is a favoured microstructure, since it is the phase which produces the highest hardness and strength in steels [1]. It is produced from austenite during rapid cooling, and the properties of the formed martensite depend greatly on the properties of austenite prior to quenching. Therefore, studying austenitization during heating is as important as examining the subsequent martensite reaction during cooling.

Austenitization occurs when the temperature of the material exceeds its characteristic austenitization temperature. The temperature at which austenite starts to form is the Ac_1 temperature. In higher temperatures the volume fraction of austenite increases at the expense of other phases, until the material is fully austenitic. The temperature at which the transformation of hypo-eutectoid steel to austenite is complete is the Ac_3 temperature. Ac_1 temperature increases slightly with increasing heating rate. This movement is quite insensitive to carbide distribution and carbon content. In contrast to the elevation of the Ac_1 temperature, the Ac_3 temperature is structure sensitive and varies considerably with the heating rate. [2]

The austenitization sequence and the resulting hardened microstructure depend on the processing parameters as well as the initial microstructure of the material. In plain carbon and low alloy steels the distribution of carbon has the greatest effect on phase transformations.

Initial Microstructure of Ferrite and Pearlite Ferrite-pearlite steels comprise microstructures of ferrite and pearlite. Pearlite is a lamellar mixture of ferrite and cementite. Therefore, the phase transformations in these steels depend on transformations occurring in the pearlitic regions as well as the transformations occurring in the ferritic regions.

If the austenitization temperature is below the austenitization temperature of ferrite, austenitization begins by transformation of pearlite grains into austenite, followed by volume diffusion of carbon to the ferritic regions leading to the growth of austenitic regions by the expense of remaining ferrite. [3]

In laser transformation hardening, in which temperatures are well above the Ac_1 temperature of ferrite, austenitization of ferrite-pearlite steel is assumed to occur by two simultaneous mechanisms: [4] In pearlite; shrinkage of the ferritic regions, controlled by volume diffusion of carbon in austenite, over a characteristic diffusion distance, taken to be half of the interlamellar spacing, and in ferrite; growth of austenite nucleated at the internal ferrite grain boundaries. The extent of following martensite reaction depends on the volume diffusion of carbon from the formerly pearlitic regions to the low carbon regions of former ferrite, as illustrated in Figure 2. Regions with low carbon content transform to pro-eutectoid ferrite.

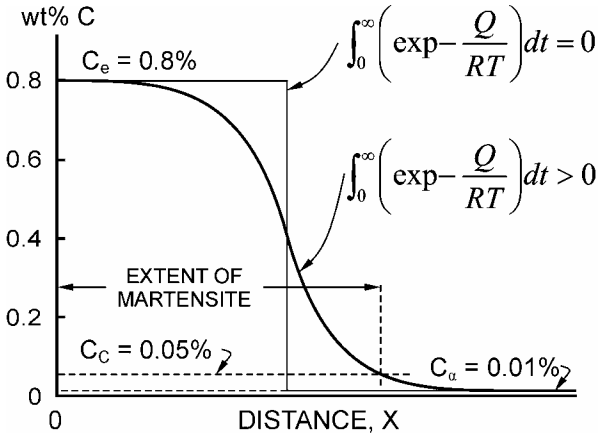

Figure 2. Diffusion profile during homogenization. [5]

Just after α → γ transformation has completed the formed austenite is still inhomogeneous [6]. Provided that the material is held at a temperature, where atomic migration is possible, and preferably fast, the solute atoms are redistributed until the austenitized material becomes uniform in composition (Fick's law). [7] Homogenization depends on the initial microstructure and the distribution of carbon in the microstructure. Austenitization and homogenization may be controlled by adjusting processing parameters. The increase of the traverse rate will result in a high heating rate and a short time above the austenitizing temperature. Decrease of the traverse rate will result in a slow heating rate and a prolonged austenitizing time. However, due to the principle of laser transformation hardening, the heating rate is always related to the cooling rate. A slow heating rate will produce a more homogenous microstructure, but the cooling rate will also be slow. Slow cooling may lead to production of softer microstructures. Homogeneity may be increased by cyclic treatment, without losing severity of quenching [8].

Austenitization of tempered martensite If no limitations apply, the favourable initial microstructure of laser hardened components is tempered martensite. In this microstructure carbon is in solution in the

matrix or in fine carbides, which are fairly uniformly distributed in the microstructure. There is no such need of carbon migration to achieve complete austenitization like in steels consisting of ferrite and pearlite. If the fine carbides consist of cementite, they are easily dissolved and the carbon is liberated to diffuse in the matrix. The material may be austenitized by extremely rapid thermal cycles and a very fine austenite grain size is achieved. However, if strong carbide forming elements, such as vanadium, are present, the alloy carbides may be uninfluenced [9].

Austenite grain size Grain growth of austenite is a diffusion-controlled process depending on the austenitization time and temperature. Therefore, the austenite grain size is largest near the surface, where the peak temperature is highest during the thermal cycle and the austenitization time is at its maximum. The grain size is at maximum at the surface and minimum in the transition zone, where austenite has just formed in temperatures near the Ac_1 temperature. [9]

Austenite grain size affects the hardness of martensite, since the austenite grain size controls the size of the martensite laths or plates formed immediately below M_s. [10] Finer grained martensite is produced from fine grained austenite. Therefore, high traverse rate or a low austenitizing temperature leads to fine grained austenite thus resulting in harder martensite. [9]

Objective

The aim of this work was to study phase transformations in steels with different initial microstructures and establish the effect of processing parameters on austenitization and the following hardened microstructure. DIC imaging was used for examining phase transformations and the microstructure of the hardened steel.

Experimental procedure

Laser Processing

A high power diode laser was used for hardening. The laser comprised stacks of separate diodes delivering radiation at wavelengths of 800±10 nm and 940±10 nm. For each power level, half of the delivered laser power comprised 800 nm radiation and half 940 nm radiation. The maximum nominal power of the laser was 3000 W. The time to attain full power was 10 ms, and the time from full power to power-off was also 10 ms. Focal length of the optic was 500 mm and the measured spot size, calculated from the second moment, was 5.3 mm in the traverse direction and 12.3 mm across the traverse direction. Figure 3 shows the measured intensity profile of the beam.

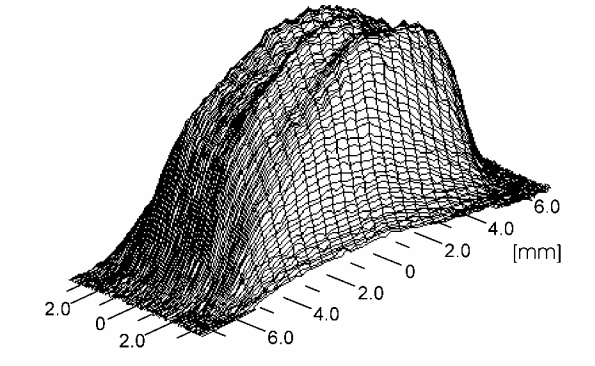

Figure 3. Measured intensity profile of the hardening optic.

Trials were made in a gas chamber in a non-oxidising atmosphere of argon. The beam was delivered to the work piece through a P270 optical glass window. The beam power at the work piece was measured with a laser power and energy meter, and represented 87% of the nominal laser power. The laser was mounted on a six-axis industrial articulated robot. The angle between the laser's optical axis and the surface was set to 85 degrees to reduce the amount of power reflected back to the laser.

The experimental set-up is illustrated in Figure 4.

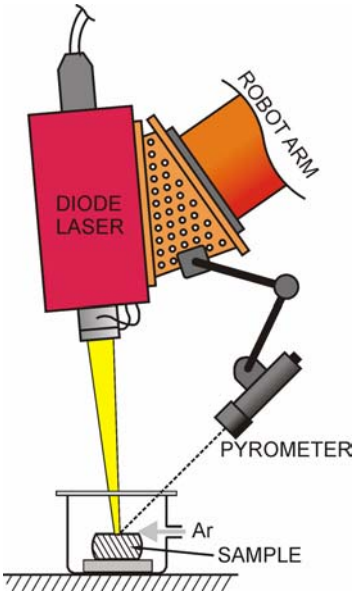

Figure 4. Schematic illustration of the experimental setup for laser processing.

Surface temperature was measured and controlled in real-time using a dual wavelength pyrometer system,

which adjusted the laser power during processing. The operable temperature range was between 761 and 1873 K. Emitted radiation was measured at wavelengths of 1300 and 1700 nm. The pyrometer was aligned to measure the peak temperature of the surface.

Test materials

Plain carbon steels C45 and S355, and heat treatable low alloy steel 42CrMo4 were used in the study. 42CrMo4 was delivered in the quenched and tempered condition; C45 and S355 were delivered in the as-rolled condition. The chemical composition of the materials is given in Table 1.

Table 1. Chemical composition of the steels (wt-%).

	C	Si	Mn	Cr	Ni	Mo
S355	0.16	0.26	0.96	0.11	0.12	0.02
C45	0.46	0.21	0.74	0.10	0.08	0.01
42CrMo4	0.44	0.34	0.70	1.10	0.16	0.18

Hardness of S355 prior to hardening was 161 HV, hardness of C45 was 199 HV and the hardness of 42CrMo4 was 312 HV. Test pieces of length 50 mm and thickness 20 to 40 mm were diamond polished and cleaned with ethanol. A hardened track of length 40 mm was produced on the surface in an inert gas atmosphere of argon.

Processing parameters

To examine the effect of processing parameters on phase transformations, test materials were hardened with different processing parameters. Traverse rate was set to 5 or 10 mm s^{-1}. Real-time process control maintained the peak surface temperature at a fixed value during each experiment. Temperature was varied between experiments from 1273 to 1673 K.

Measuring equipment

Micrographs of as-processed surfaces were taken using an optical microscope with DIC (Differential Interference Contrast) optics, which reveals the surface relief caused by the shape change during phase transformations.

Hardness tests were performed for all samples using a Vickers hardness testing. Five measurements were taken from each sample with 5 mm spacing.

Results

Hardening of polished surfaces in inert gas atmosphere clearly illustrated the process of laser transformation hardening, Figure 5. Laser beam could be seen heating the surface of the material. Behind the beam is the austenitic region, which is rather smooth but shows little surface shape change. As the material quenches it transforms into martensite appearing grey in the figure. Experienced martensite transformation induces a surface relief, which reflects light differently than the polished metal surface. Phase transformations in each steel sample were examined further by studying the surface relief patterns by DIC imaging.

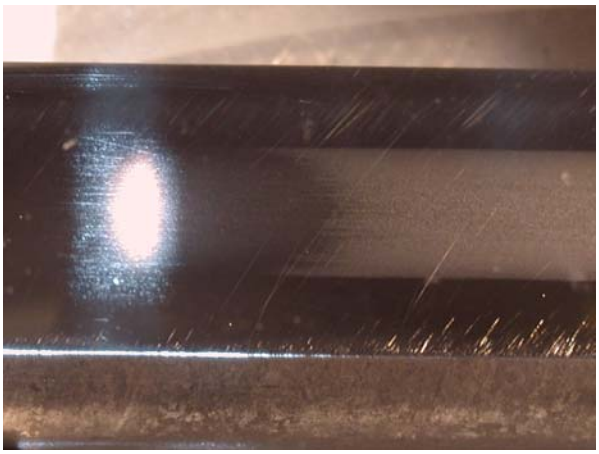

Figure 5. Image of steel surface during laser transformation hardening.

S355

The hardened track could be divided into three separate areas. Near the centre of the track was the hardened zone at which the material had austenitized completely, although the austenite might not have been homogeneous. On both sides of the hardened track a transition zone could be noticed. In this zone pearlite grains have austenitized, but the ferritic regions remain as ferrite, due to the low peak temperature in this zone. Out side of the transition zone is a region which has not austenitized during processing, but the surface has not remained smooth. It can be assumed that in this region the surface shape change is due to stress relief and grain coarsening. The surface geometry of the transition zone is presented in Figure 6. The hardness in this zone increased only 59 HV compared to the base material. Image taken from the centre line of the same sample shows similar phases, martensite and ferrite, Figure 7. Martensitic regions are not as clearly outlined as in the transition zone. Hardness measured from the centre line was 296 HV.

The traverse rate was decreased to allow more carbon diffusion during austenitization. Surface hardness was increased to a value of 323 HV when the traverse rate was 5 mm s^{-1} and the peak temperature was 1273 K. Increasing the peak surface temperature to 1473 and

1623 K produced surface hardness of 410 and 423 HV, respectively. Surface processed with a traverse rate of 5 mm s^{-1} and a peak temperature of 1473 K is presented in Figure 8. Martensite covered considerably larger areas of the surface than in Figures 6 and 7. The boundaries between martensitic and ferritic regions were not clear. Pre-austenite grain boundaries are visible.

C45

Similar zones as in the hardened track of S355 samples could be found in the C45 samples. The hardness was increased considerably even in the transition zone; from 199 HV of the base material up to 440 HV. The transition zone consisted of untransformed ferrite and martensite formed from the austenitized pearlite. Ferrite bands are visible as smooth areas between the martensitic regions in Figure 9. Ferritic and martensitic regions could not be clearly identified at the centre line of the hardened track even from the samples processed with the lowest processing temperatures. Surface of a sample processed with 10 mm s^{-1} traverse rate and 1273 K peak temperature is illustrated in Figure 10. Surface hardness was increased to 715 HV.

When traverse rate was decreased to 5 mm s^{-1} surface hardness was increased to approximately 750 HV. No significant variation in the hardness was detected with variation of the surface temperature. A marked increase in the martensite grain size was observed with increasing surface temperature. Figures 11 and 12 illustrate the effect of surface temperature on the martensite grain size. It should be noted that raising surface temperature affects also the austenitization time, since more time is required for thermal conduction.

42CrMo4

42CrMo4 steel was delivered in the quenched and tempered condition and no such redistribution of carbon was required during austenitization as when hardening steels containing ferrite and pearlite. Surface hardness of all processed samples was between 761 and 778 HV. The most significant effect of the processing parameters was the effect on grain size. Faster grain size and lower peak temperature produced very fine grained martensite, as presented in Figure 13, whereas a slow traverse rate and a high surface temperature induced coarsening of austenite grains and subsequent increase in the martensite grain size, Figures 14 and 15.

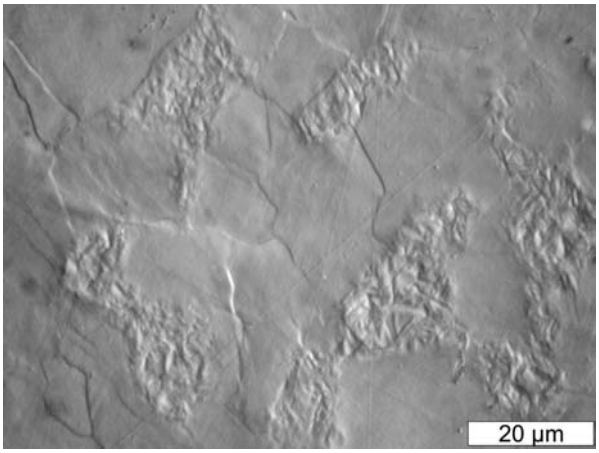

Figure 6. Surface geometry of transition zone in S355. Traverse rate 10 mm s^{-1}. Surface hardness 220 HV.

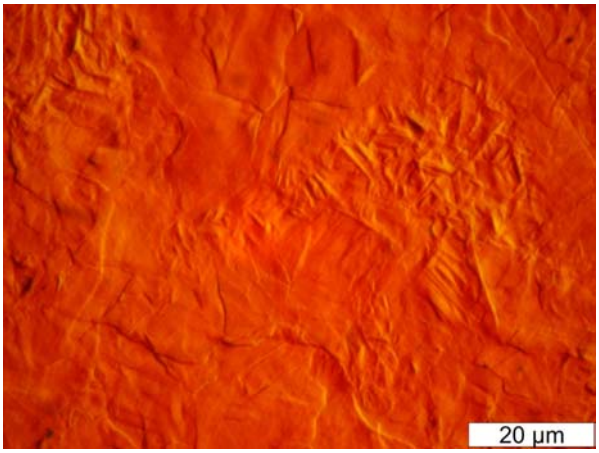

Figure 7. Surface geometry at the centre line of the hardened track in S355. Traverse rate 10 mm s^{-1}, peak temperature 1273 K. Surface hardness 296 HV.

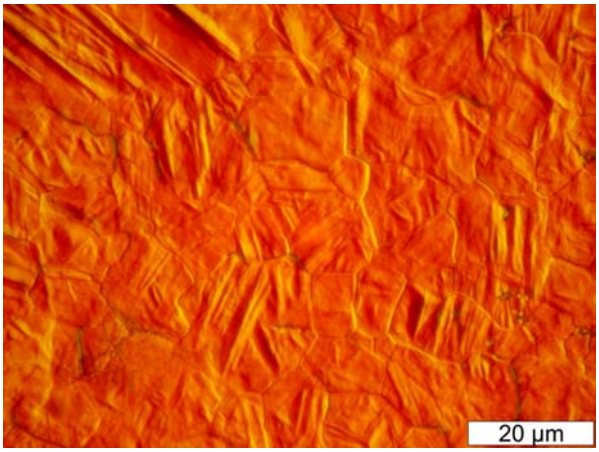

Figure 8. Surface geometry at the centre line of the hardened track in S355 steel. Traverse rate 5 mm s^{-1}, peak temperature 1473 K. Surface hardness 410 HV.

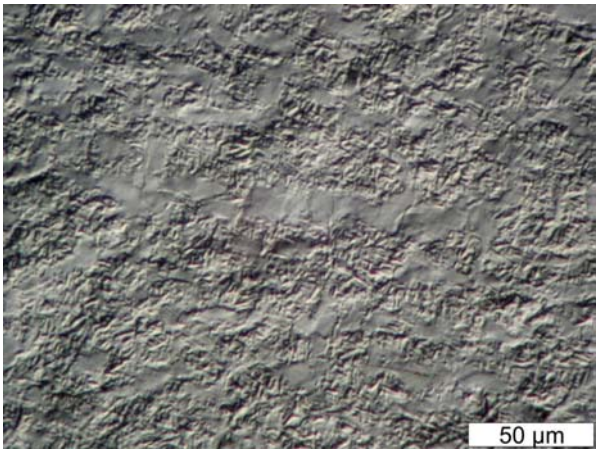

Figure 9. Transition zone of C45 sample. Traverse rate 10 mm s^{-1}.

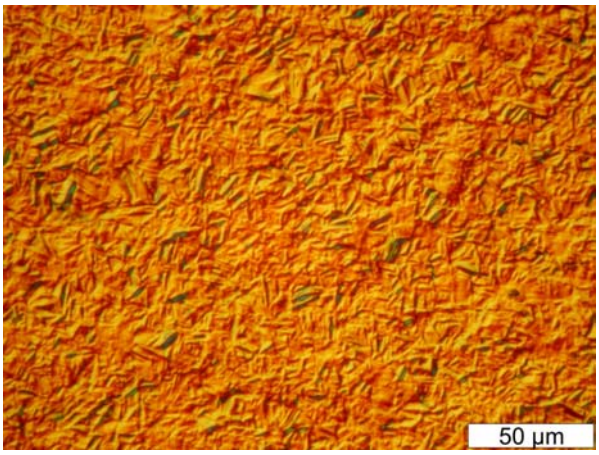

Figure 10. Surface geometry at the centre line of the hardened track in C45 steel. Traverse rate 10 mm s^{-1}, peak temperature 1273 K. Surface hardness 715 HV.

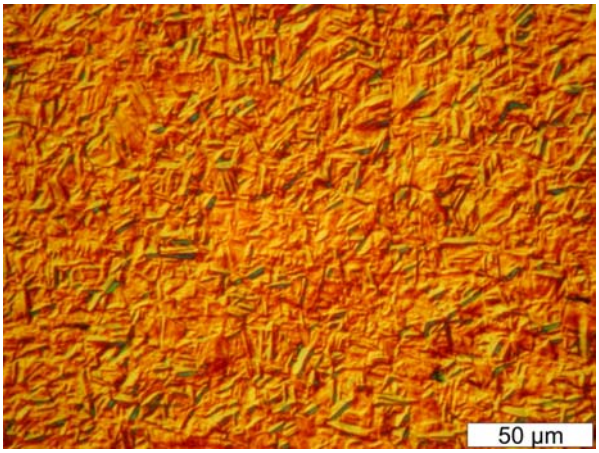

Figure 11. Surface geometry at the centre line of the hardened track in C45 steel. Traverse rate 5 mm s^{-1}, peak temperature 1273 K. Surface hardness 744 HV.

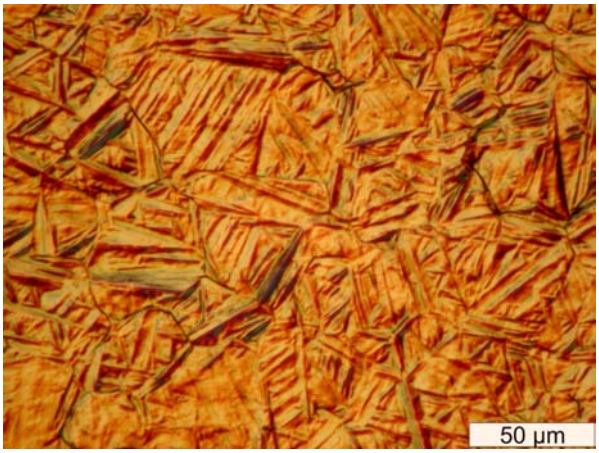

Figure 12. Surface geometry at the centre line of the hardened track in C45 steel. Traverse rate 5 mm s^{-1}, peak temperature 1603 K. Surface hardness 748 HV.

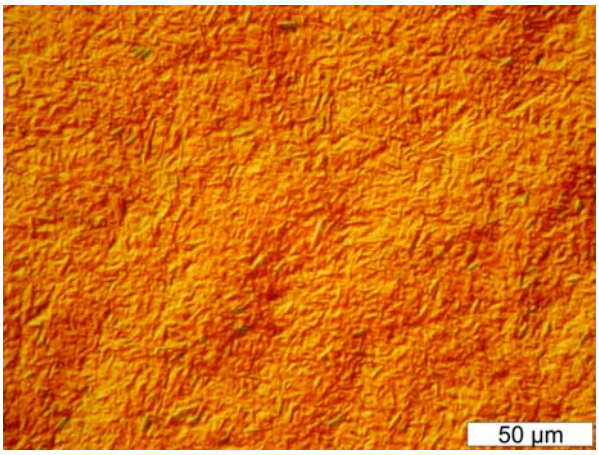

Figure 13. Surface geometry at the centre line of the hardened track in 42CrMo4. Traverse rate 10 mm s^{-1}, peak temperature 1273 K. Surface hardness 767 HV.

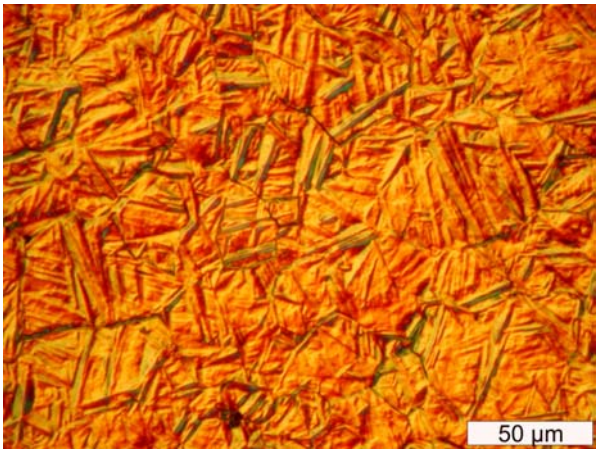

Figure 14. Surface geometry at the centre line of the hardened track in 42CrMo4. Traverse rate 5 mm s^{-1}, peak temperature 1673 K. Surface hardness 748 HV.

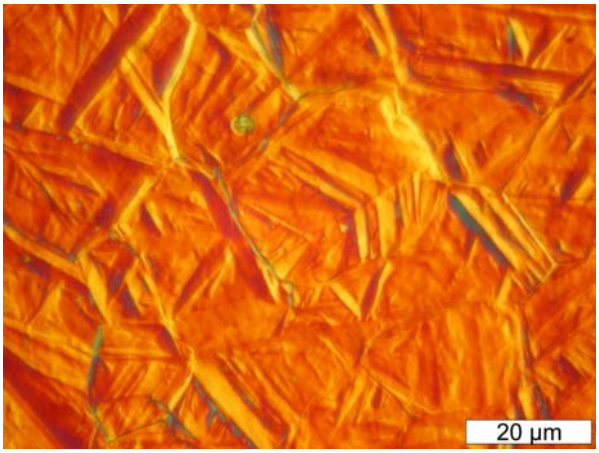

Figure 15. Surface geometry at the centre line of the hardened track in C45 steel. Traverse rate 5 mm s^{-1}, peak temperature 1673 K. Surface hardness 748 HV.

Discussion

S355 samples clearly present the effect of processing parameters on austenitization of ferrite-pearlite steels. Lowest austenitization temperatures, namely in the transition zone, produce a microstructure of martensitic areas formed from austenitized pearlite in a matrix of ferrite. The areas are very sharply outlined, as seen in figure 6. Pearlite grains have austenitized, but low temperature and short austenitization time do not allow volume diffusion of carbon into the surrounding ferrite. Therefore only the formerly pearlitic areas are transformed into martensite.

Higher surface temperature enables austenitization of ferritic regions regardless of carbon diffusion. Higher temperature also increases the diffusion rate. Austenite formed from pearlite grains acts as a source of carbon. Increased diffusion rate enables a longer diffusion distance during the thermal cycle. Consequently, increased amount of austenite is provided with adequate quantities of carbon for martensitic transformation. The volume fraction of martensite increases at the expense of pro-eutectoid ferrite, Figures 7 and 8. The boundary between martensite and ferrite becomes indistinct. Decreasing the traverse rate and thus prolonging the time above the austenitization temperature has a similar effect on carbon diffusion.

Surface hardness was found to increase with higher surface temperature and longer austenitization time. When carbon diffusion is insignificant martensite produced from austenitized pearlite has a carbon content of approximately 0.8 wt-%. Such high carbon martensite is hard, but since the volume fraction of martensite is minor, only a slight increase in the hardness of the material is achieved. Hardening with processing parameters which allow greater amount of carbon diffusion, increases the amount of martensite in the structure. Formed martensite has lower carbon content and therefore is softer, but the volume fraction of martensite is larger, thus producing a harder surface. Hardest surface, 421 HV, was achieved with a peak surface temperature of 1623 K and a traverse rate of 5 mm s^{-1}.

Homogeneous austenite may be produced, if the traverse rate is sufficiently slow and the austenitization temperature is high. However, such processing parameters will also induce a low cooling rate, and softer microstructures may form.

C45 has higher carbon content than S355 and therefore the initial microstructure contains more pearlite. From figure 9 it can be seen that in the transition zone, in which carbon diffusion is insignificant, martensite formed from austenitized pearlite covers over half of the microstructure. Hardening with a peak surface temperature of 1273 K and a traverse rate of 10 mm s^{-1} produced a fully martensitic microstructure, Figure 10. Highest hardness was achieved with traverse rate being 5 mm s^{-1}. Surface temperature did not have an effect on the hardness, but Figures 11 and 12 clearly show a difference of martensite lath size. Martensite grain size depends on the austenite grain size from which it is formed. Austenite grain growth is a diffusion limited process and therefore a longer austenitization time and higher surface temperature encourages growth of austenite grains, subsequently producing coarser grained martensite.

Due to the fairly uniform distribution of carbon in the quenched and tempered 42CrMo4, austenite formed during heating is assumed to be homogeneous and the material becomes fully martensitic after quenching. Processing parameters have the greatest effect on martensite grain size. However it should be noted that the hardness of martensite is very similar in all samples and with examined processing parameters martensite lath size did not have significant effect on the hardness of martensite.

Conclusions

Hardening of polished surfaces in an inert gas atmosphere provides useful data of phase transformations during laser transformation hardening. Phase transformations and microstructure of the hardened material can be examined with DIC imaging. Extent of martensite, pre-austenite grain size and martensite lath size can be measured from DIC images. However, classification of phases may be difficult since for example bainite is formed by quite similar shear process than martensite and the surface relief of bainite may be similar to that of martensite.

Extent of martensite depends on the processing parameters and the initial microstructure. Steels with a higher pearlite fraction or a microstructure, in which carbon is distributed uniformly, may be hardened with higher traverse rates and lower austenitization temperatures than low carbon steels consisting mainly of ferrite.

Highest hardness is achieved when the extent of martensite is increased by allowing sufficient carbon diffusion. Pre-austenite grain size was not found to have a significant effect on the hardness with examined processing parameters.

Acknowledgements

This study was done as a part of the project 'Intelligent Laser Surface Engineering', funded by the Academy of Finland for the years 2000-2003.

References

[1] Krauss, G. (1990) Microstructures, processing and properties of steels, in. Metals Handbook, vol. 1, 10th Ed., American Society of Metals, 126-139.

[2] Albutt, K.J., Garber, S. (1966) Effect of heating rate on the elevation of critical temperatures of low-carbon mild steel. Journal of The Iron and Steel Institute, 1217-1222.

[3] Karlsson, B. (1972) Transformation kinetics for the formation of austenite from a ferritic-pearlitic structure, Z. Metallkde 63, 160-164.

[4] Ion, J.C; Moisio, T.J.I; Paju, M; Johansson, J. (1992) Laser transformation hardening of low alloy hypoeutectoid steel, Materials Science and Technology 8, 799-803.

[5] Ashby, M.F; Easterling, K.E. (1984) The transformation hardening of steel surfaces by laser beams – I. Hypoeutectoid steels, Acta Metallurgica 32 1935-1948.

[6] Li, W-B; Easterling, K.E; Ashby, M.F. (1986) Laser transformation hardening of steel – II. Hypereutectoid steels, Acta Metallurgica 34, 1533-1543.

[7] Smallman, R.E; Bishop, R.J. (1999) Modern Physical Metallurgy, 6th Ed., Butterworth-Heinemann, 438 p.

[8] Bernshteyn, M.L; Prokoshkin, S.D; Kaputkina, L.N; Kal'ner, Yu.V; Bernshteyn, A.M. (1989) X-ray diffraction examination of the structure of carbon steels after laser heat treatment, Phys. Met. Metall. 67, 128-135.

[9] Obergfell, K; Schultze, V; Vöhringer, O. (2003) Classification of microstructural changes in laser hardened steel surfaces, Materials Science and Engineering A355, 348-356.

[10] Pickering F.B. (1978) The optimization of microstructures in steel and their relationships to mechanical properties, in Doane, D.V; Kirkaldy, J.S. (eds) Hardenability Concepts with Applications to Steel, American Institute of Mining and Metallurgical Engineers, 179-225.

Meet the author

Henrikki Pantsar is a Research Scientist and a Dr. (tech.) student in the Laser Processing Laboratory of Lappeenranta University of Technology. His doctoral research focuses on the mathematical modelling of laser transformation hardening.